coatings

MDPI

Article

Effect of Atomic-Layer-Deposited Hydroxyapatite Coating on Surface Thrombogenicity of Titanium

Faleh Abushahba [1,2,3,*], Nagat Areid [1], Elina Kylmäoja [4], Jani Holopainen [5], Mikko Ritala [5], Leena Hupa [6], Juha Tuukkanen [4] and Timo Närhi [1,7]

1 Department of Prosthetic Dentistry and Stomatognathic Physiology, Institute of Dentistry, University of Turku, 20520 Turku, Finland; nmaare@utu.fi (N.A.)
2 Department of Biomaterials Science and Turku Clinical Biomaterial Center-TCBC, Institute of Dentistry, University of Turku, 20520 Turku, Finland
3 Department of Restorative Dentistry and Periodontology, Faculty of Dentistry, Libyan International Medical University (LIMU), Benghazi 339P+62Q, Libya
4 Department of Anatomy and Cell Biology, Institute of Cancer Research and Translational Medicine, Medical Research Center, University of Oulu, 90014 Oulu, Finland
5 Department of Chemistry, University of Helsinki, 00014 Helsinki, Finland
6 Johan Gadolin Process Chemistry Center, Åbo Akademi University, 20500 Turku, Finland
7 The Wellbeing Service County Southwest Finland, 20521 Turku, Finland
* Correspondence: fafabu@utu.fi

Abstract: This study aimed to evaluate the surface characteristics of a nanocrystalline hydroxyapatite coating made through atomic layer deposition (ALD-HA) on titanium surfaces and to investigate its effect on blood coagulation and platelet adhesion. Grade 2 square titanium discs (0.7 cm, 1 mm thick) were used (n = 108). Half of the substrates (n = 54) were coated with ALD-HA, and the other half were used as the non-coated control. Surface free energy (SFE), contact angle (CA), surface roughness (Ra), and chemical composition were evaluated. Blood thrombogenic properties were assessed on ALD-HA and non-coated surfaces using the kinetic clotting time method. The platelets' adhesion and morphology were also evaluated. The ALD-HA-coated surfaces demonstrated significantly higher polar SFE ($p < 0.001$) and lower CA ($p < 0.001$) values compared to the non-coated surfaces. In addition, the surface roughness was significantly lower for the ALD-HA ($p < 0.001$) than for the non-coated surfaces. Platelets adhered to both surfaces; however, there was variability in platelet morphologies in different areas with higher platelet density on the ALD-HA surfaces. There was no significant difference in the overall absorbance values of the hemolyzed hemoglobin for both substrates, and the total clotting time was achieved at 60 min. It can be concluded that the ALD-HA coating of titanium can enhance surface wettability, increase surface free energy, and support blood coagulation and platelet adhesion.

Keywords: ALD; platelets adhesion; blood coagulation; hydroxyapatite coating; titanium

Citation: Abushahba, F.; Areid, N.; Kylmäoja, E.; Holopainen, J.; Ritala, M.; Hupa, L.; Tuukkanen, J.; Närhi, T. Effect of Atomic-Layer-Deposited Hydroxyapatite Coating on Surface Thrombogenicity of Titanium. *Coatings* **2023**, *13*, 1810. https://doi.org/10.3390/coatings13101810

Academic Editor: Lech Pawlowski

Received: 8 September 2023
Revised: 19 October 2023
Accepted: 20 October 2023
Published: 22 October 2023

1. Introduction

Modifications to implant surfaces are intended to increase osseointegration [1]. Various modification techniques, including additive and subtractive, have been used to modify the surface properties of titanium implant surfaces [2]. The surface properties, such as topography, chemical composition, and roughness, are crucial factors that influence the biological responses at the bone–implant interface and, consequently, osseointegration [1,3].

The hydroxyapatite (HA) implant coating has been extensively investigated and has shown a higher efficiency than uncoated titanium due to the direct growth of bone tissue onto the HA coating [4,5]. Several coating methods and techniques have been used to form calcium phosphate layers on titanium surfaces, such as laser deposition, sputter coating, electrophoretic or sol–gel deposition, and plasma spraying. Plasma spray coating has been

intensively investigated, and this technique can produce a coating thickness on titanium between 30 and 200 µm [6]. In vivo studies have shown that this coating can provide strong osteoconduction effects [5,7]. Despite its strong osteoconductive properties, several problems are associated with this method, such as flaking, brittleness, and delamination [8,9]. These problems are caused by the low cohesive strength and high processing temperature, resulting in inhomogeneity of the chemical composition [10,11]. Atomic layer deposition (ALD) is a method that can overcome these issues and produce nano-scale coatings with controlled thickness on complex three-dimensional surfaces [12].

Holopainen et al. [13] described a method that can be used to produce a very thin, uniform layer of nanocrystalline HA through atomic layer deposition (ALD-HA). Avila et al. [14] investigated the thickness and the mechanical properties of layers produced over 2000 and 4000 cycles. Both cycles yielded a nano-thickness hydroxyapatite layer (300 nm for the 2000 and 380 nm for the 4000 cycles) and showed good adhesion strength to titanium surfaces up to 6.71 MPa with alkaline conversion solution. Thus, this coating can potentially minimize the risks associated with the HA layer produced using the other methods and improve implant survival. Good mechanical anchorage is a crucial feature of implant surfaces that promote integration with the surrounding bone [15].

Previous studies indicated that osteoblast cell adhesion and viability on ALD-HA deposited on titanium substrates are comparable to bone [16]. However, the human peripheral blood monocytes differentiate in different manners on ALD-HA and bone [17]. On the bone, osteoclastogenesis was induced, and the multinuclear cells were able to resorb the bone. On the ALD-HA, by contrast, a foreign body reaction was noticed, and the cells lacked the resorption capacity [17].

After surgical placement of an implant, favorable interaction between the implant surface and blood system is crucial in determining implant success. This interaction begins immediately after implant insertion through clot formation around the implant, representing the connection site between the implant surface and the surrounding tissues and initiating the peri-implant tissue healing process [18,19]. Any chemical modification on the implant surface may interfere with the blood coagulation cascade and platelet adhesion and affect the early event of wound healing around implant surfaces. To the authors' knowledge, the blood and platelet responses on the ALD-HA surfaces have not been studied. Therefore, this study aimed to examine the surface characteristics of ALD-HA deposited on titanium surfaces and to evaluate its effect on blood coagulation and platelets response.

2. Materials and Methods

2.1. Preparation of Nanocrystalline Hydroxyapatite Coating on Ti Discs

The preparation of ALD-HA coatings has been described elsewhere [13,20]. In short, a 1 mm thick titanium sheet (Grade 2, ASTM B265 specification, William Gregor Ltd., London, UK) was used as a substrate. The ALD-HA coating was made by first depositing a thin film of $CaCO_3$ in an F-120 ALD reactor (ASM Microchemistry Ltd., Helsinki, Finland) using $Ca(thd)_2$ and O_3 as precursors. The $Ca(thd)_2$ (Volatec Oy, Porvoo, Finland) was evaporated at 188 °C and O_3 was generated from O_2 (99.9999%) using a Wedeco Ozomatic Modular 4 HC Lab ozone generator. The depositions were conducted at 250 °C with 2000 ALD cycles. Subsequently, the $CaCO_3$ film was converted to HA in 0.2 M $(NH_4)_2HPO_4$ (Merck, 99%, Darmstadt, Germany) solution at 95 °C. The samples were finally rinsed with deionized water, dried with compressed air, and cut into 0.7 × 0.7 cm^2 discs using a manual plate cutter (Bernardo PTS 1050 S Manual disc cutter, Linz, Austria).

2.2. Surface Roughness Measurements

The surface roughness averages of the ALD-HA-coated and the non-coated titanium samples were measured using a 3D non-contact optical profilometer (Bruker Nano GmbH, Billerica, MA, USA) using a 5× objective lens and a 0.5 multiplier. Vision 64 software was

used to calculate surface areas and roughness parameters, represented by the mean Ra values of roughness measured at six randomly selected locations.

2.3. Water Contact Angle (CA) Measurements

The surface wettability of the ALD-HA and non-coated titanium substrates was evaluated from CA measurements using the sessile drop method described by Jong et al. [21] using a contact angle meter (KSVCAM100 KSV, Instrument LTD, Espoo, Finland). The Young–Laplace equation was applied to determine the CA on the substrates. A drop of distilled water was deposited on the substrate's surface, and 140 images were captured in 10 s at room temperature (n = 6). The mean value of the CA on both sides of the droplet was calculated.

2.4. Surface Free Energy (SFE) Calculations

The SFE was calculated on the ALD-HA and non-coated titanium surfaces using the same sessile drop method as above, and the Owens–Wendt (OW) approach was applied. Three liquids were used as a probe to evaluate the SFE: distilled ultrapure water, diiodomethane (>99% purity), and formamide (>98% purity). The mean value of 6 drops on each specimen for each liquid was calculated, and the results are expressed as total (γtot), dispersive (γd), and the polar (γp) SFE components.

2.5. Scanning Electron Microscopy (SEM) and Energy-Dispersive X-ray Spectroscopy (EDS) Analysis

SEM images and EDS analysis of the ALD-HA-coated and uncoated titanium surfaces were performed using scanning electron microscopy (LEO Gemini 1530, Carl Zeiss, Oberkocken, Germany) and an X-ray detector (Thermo Scientific, Waltham, MA, USA).

2.6. Clotting Time Measurements

The thrombogenic properties of the titanium substrates were assessed using a whole blood kinetic clotting time method [22]. A total of 90 substrates were used. Each experimental group (ALD-HA and the non-coated) had 45 substrates. The fresh blood was obtained from three healthy non-smoker volunteers (among the research group) with venipuncture using disposable syringes. The first drawn 3 mL of blood was disposed of to prevent possible thromboplastin contamination caused by needle puncture. Then, 0.05 mL of the obtained blood was immediately pipetted on the substrate in 12-well plates, followed by adding 1.5 mL of distilled water at a predetermined time of 10, 20, 30, 40, and 60 min at room temperature. After 5 min, triplicate samples were taken from each well and transferred to a 96-well plate. A spectrometer was used to colorimetrically measure the released hemoglobin from the lysed red blood cells in the distilled water at 570 nm absorbance. Three technical replicates (n = 3) were used for each time point per group.

2.7. Platelet Adhesion Test

This test evaluated the platelets' morphology and adhesion behavior on the ALD-HA and the non-coated titanium substrates. Fresh human blood was obtained from three healthy, non-smoker volunteers as described in the above test. An anticoagulant (0.109 M solution of sodium citrate) was added to the blood at a 9:1 dilution ratio (blood/sodium citrate solution) and then centrifuged at 1500 rpm for 15 min to obtain platelet-rich plasma (PRP). Then, 50 µL of the obtained PRP was carefully pipetted on each substrate (three technical replicates per group per donor were used) and incubated at 37 °C for 1 h. The samples were then rinsed thrice with phosphate-buffered saline (PBS) and fixed with 2.5% glutaraldehyde solution for 2 h. Finally, the samples were rinsed in PBS and dehydrated in an alcohol series with concentrations of 70%, 95%, 99%, and 100%. The dried substrates with platelets were carbon-sputter-coated before imaging using Emscope TB 500 Temcarb. The platelet morphology was assessed through SEM based on qualitative analysis at randomly selected fields.

2.8. Statistical Analysis

The distributions of statistical variables were studied and described. Measurements are reported as means and standard deviations (SD). The differences between the experimental treatments were evaluated using one-way ANOVA (analysis of variance) at an alpha level of 5%, which indicates the maximum risk of rejecting the null hypothesis. The results were determined to be significant at p-value < 0.05. Statistical analyses were performed using the Statistical Package for the Social Sciences (SPSS) statistical software version 28.0 (SPSS Inc., Chicago, IL, USA).

3. Results

3.1. Surface Roughness, Contact Angle, and Surface Free Energy

The surface characteristics are displayed in Table 1. The surface of the ALD-HA coating demonstrated a significantly lower mean (SD) Ra value [0.69 µm (0.09); $p < 0.001$] compared to the non-coated surfaces [1.19 µm (0.06)]. The surface wettability of the ALD-HA coatings was significantly higher, as demonstrated by their lower water CA value (Figure 1).

Table 1. Mean and standard deviation of surface roughness (µm), water contact angle (°), and surface free energy determination on non-coated and ALD-HA-coated surfaces. * $p < 0.001$.

Sample	Surface Roughness (Ra)	Water Contact Angle	Surface Free Energy		
			OWTOT	OWD	OWP
Non-coated	1.19 µm (0.06)	84.65° (4.17)	36.84 (1.12)	32.52 (1.28) *	4.55 (0.94) *
ALD-HA	0.69 µm (0.09) *	76.13° (2.41) *	35.03 (2.08)	27.01 (1.54) *	8.01 (1.10) *

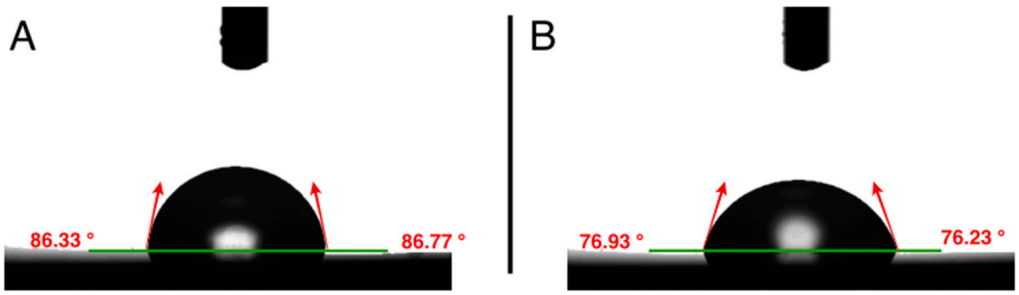

Figure 1. Water contact angle on the non-coated (**A**) and on the ALD-HA (**B**) substrates.

The total SFE values were not significantly different between the coated and non-coated substrates. However, the ALD-HA-coated surfaces displayed a significantly higher total polar (γp) SFE component compared with the non-coated surfaces ($p < 0.001$). Contrarily, the dispersive (γd) SFE component was significantly higher for the non-coated sample compared to the ALD-HA-coated surfaces ($p < 0.001$).

Figure 2 shows typical surface profiles of the non-coated and ALD-HA-coated titanium substrates.

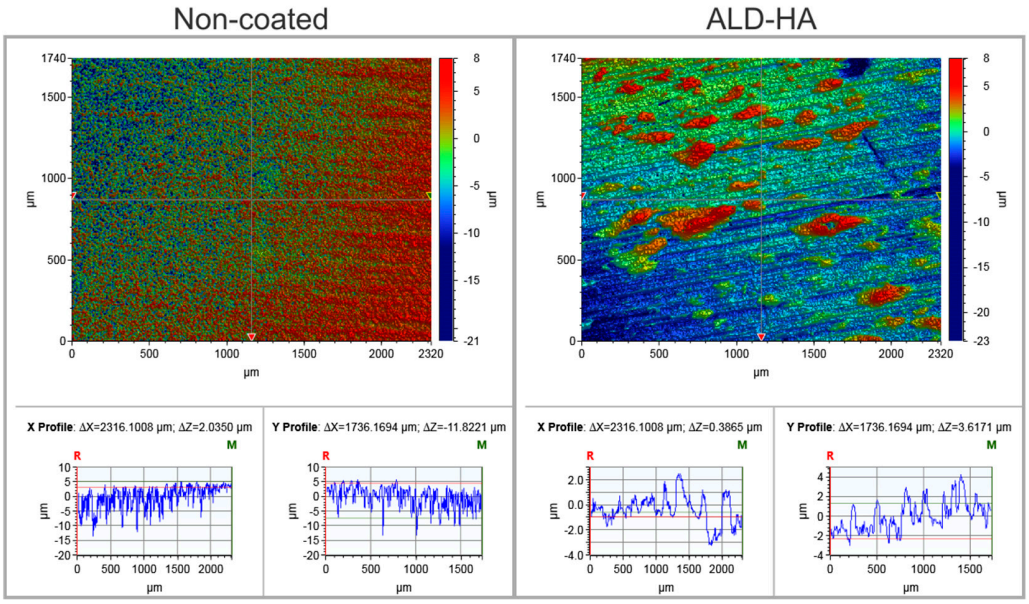

Figure 2. Typical surface profiles of the non-coated and ALD-HA-coated titanium substrates. Images show that the ALD-HA coating resulted in a smoother surface topography in both X and Y profiles compared to the non-coated substrate. Images were captured using a 5× objective lens and a field of view multiplier of 0.5×.

3.2. Scanning Electron Microscopy (SEM) and Energy-Dispersive X-ray Spectroscopy (EDS) Analysis

SEM images revealed that the non-coated titanium surface demonstrated parallel grooves, a feature of the machined surface, with almost regular surface topography (Figure 3). In contrast, HA crystals appeared and covered the entire surface of the ALD-HA-coated sample. The EDS analysis showed Ca and P on the ALD-HA-coated substrate, while mainly Ti was discovered on the non-coated surfaces (Figure 4).

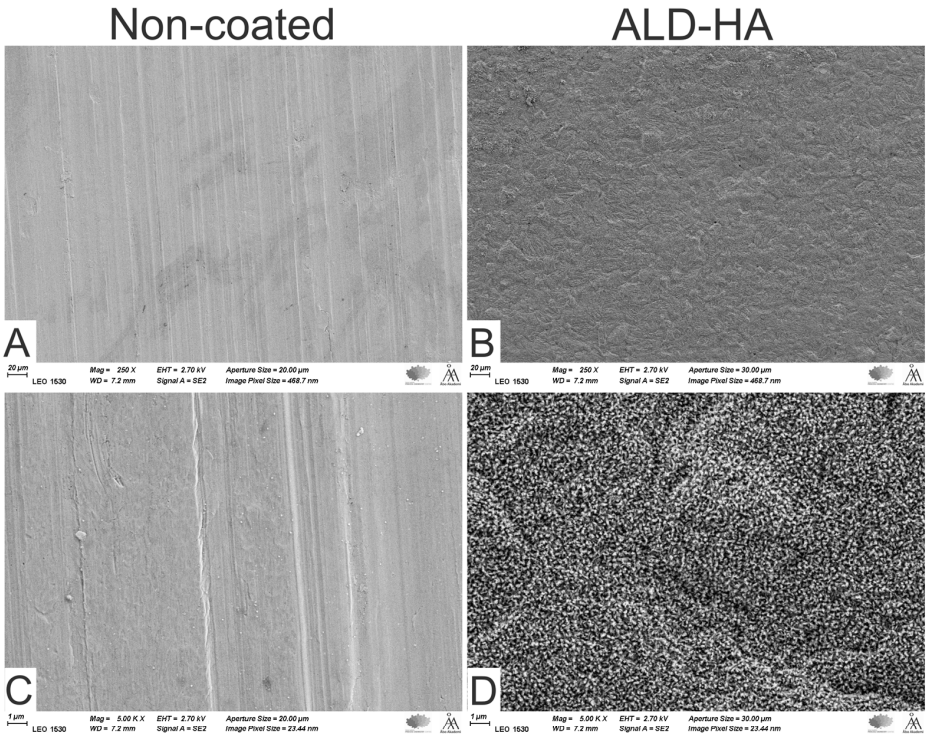

Figure 3. *Cont.*

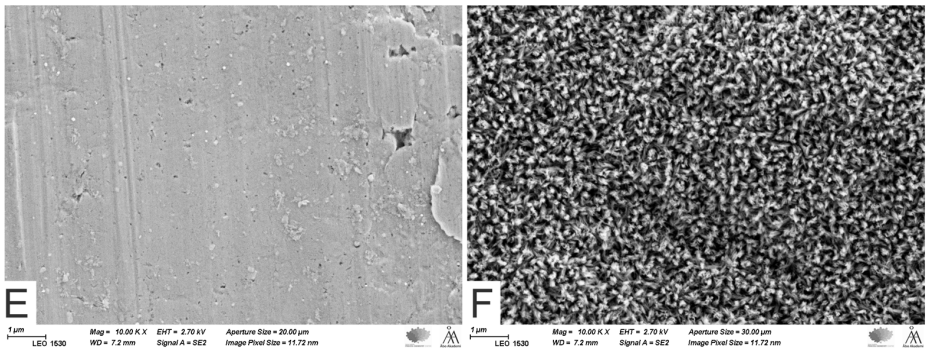

Figure 3. Scanning electron microscopic images of non-coated (**A**,**C**,**E**) and ALD-HA-coated (**B**,**D**,**F**) titanium substrates. Magnifications 250× (**A**,**B**), 5000× (**C**,**D**), and 10,000× (**E**,**F**).

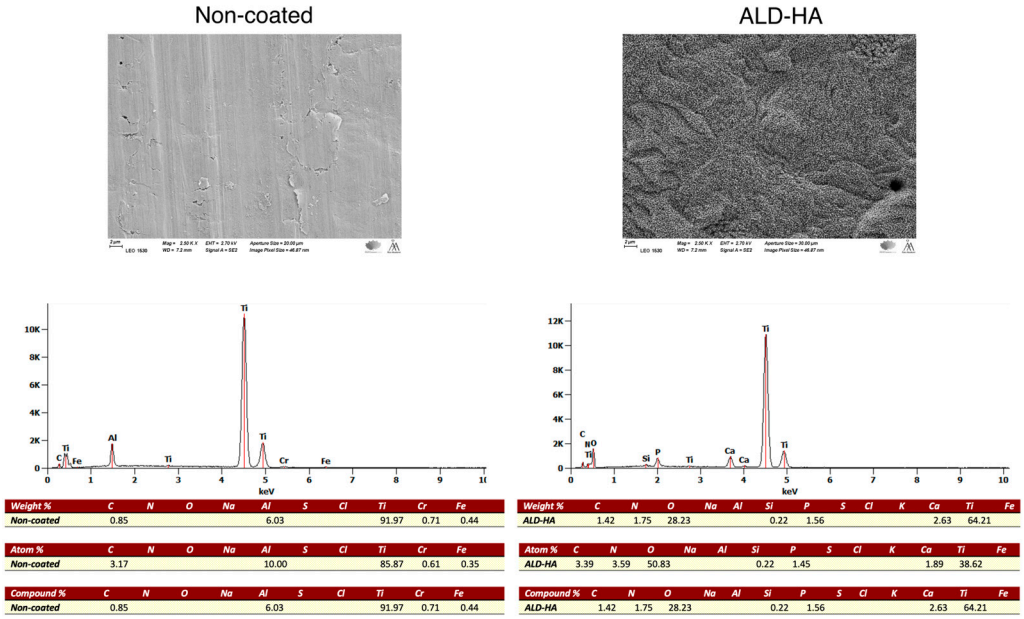

Weight %	C	N	O	Na	Al	S	Cl	Ti	Cr	Fe
Non-coated	0.85				6.03			91.97	0.71	0.44

Weight %	C	N	O	Na	Al	Si	P	S	Cl	K	Ca	Ti	Fe
ALD-HA	1.42	1.75	28.23			0.22	1.56				2.63	64.21	

Atom %	C	N	O	Na	Al	S	Cl	Ti	Cr	Fe
Non-coated	3.17				10.00			85.87	0.61	0.35

Atom %	C	N	O	Na	Al	Si	P	S	Cl	K	Ca	Ti	Fe
ALD-HA	3.39	3.59	50.83			0.22	1.45				1.89	38.62	

Compound %	C	N	O	Na	Al	S	Cl	Ti	Cr	Fe
Non-coated	0.85				6.03			91.97	0.71	0.44

Compound %	C	N	O	Na	Al	Si	P	S	Cl	K	Ca	Ti	Fe
ALD-HA	1.42	1.75	28.23			0.22	1.56				2.63	64.21	

Figure 4. Energy-dispersive X-ray spectra (EDS) of the chemical composition of the non-coated and the ALD-HA-coated titanium substrates.

3.3. Clotting Time Measurement

The overall blood clotting profiles for the non-coated and ALD-HA-coated substrates showed that the absorbance of the hemolyzed hemoglobin varied with time and was not significantly different between the non-coated and coated substrates. Complete blood clotting on both surfaces was reached in 60 min at optical density (OD) < 0.1 (Figure 5). However, the individual absorbance values vary between individual donors (Figure 6). After 20 min, Donor 3 blood showed a significantly lower mean (SD) OD value on ALD-HA and non-coated surfaces [0.96 (0.66) and 0.87 (0.09)] compared to Donor 1 [1.11 (0.12); p = 0.001 and 1.09 (0.11); p = 0.01] and Donor 2 [1.15 (0.09); p = 0.002 and 1.45 (0.14); p < 0.001]. After 30 min, the OD was not significantly different on the ALD-HA-coated surfaces, but on the non-coated surfaces, Donor 1 showed a significantly lower OD [0.45 (0.23)] compared to Donor 2 [0.76 (0.17); p = 0.004)] and Donor 3 [0.73 (0.10); p = 0.009]. After 40 min, Donor 1 demonstrated a lower OD value [0.08 (0.01)] on the ALD-HA-coated substrates than Donor 2 [0.16 (0.06); p = 0.002)] and Donor 3 [0.17 (0.04); p = 0.001]. For the non-coated substrates, both Donor 1 and 2 showed significantly lower and similar OD values [0.12 (0.03)] compared to Donor 3 [0.19 (0.06); p = 0.011]. However, complete blood coagulation on both substrates was reached at 60 min, at which the OD values were less than 0.1.

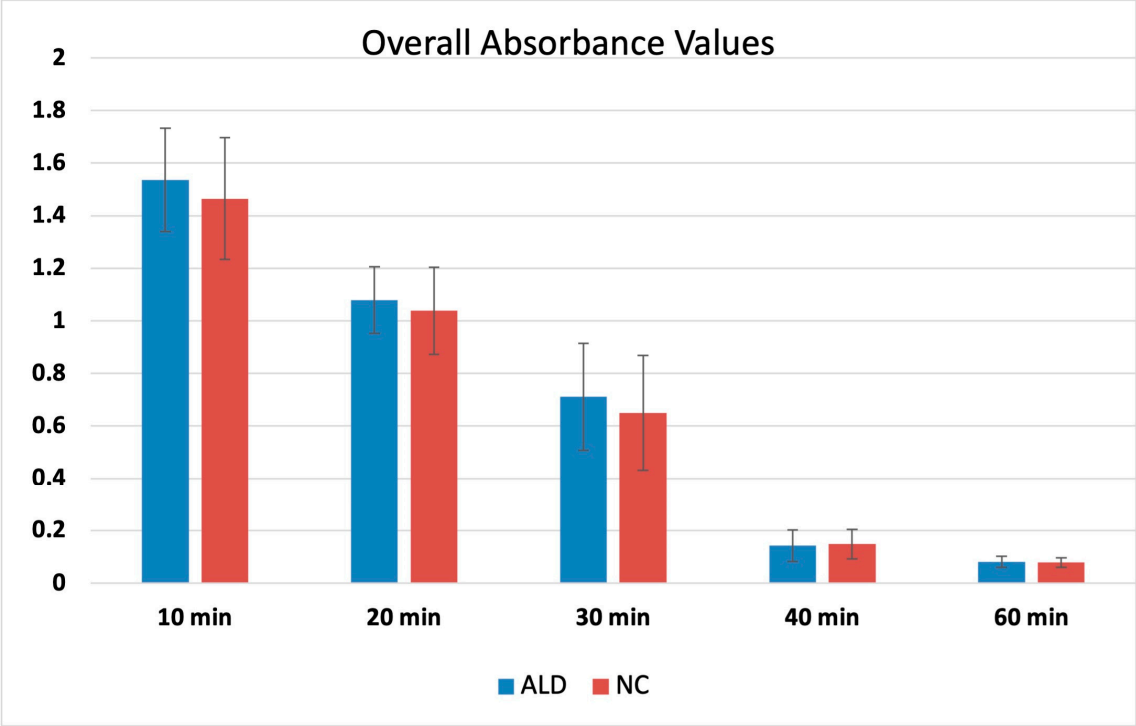

Figure 5. Mean (±SD) optical density (OD) at 570 nm vs. time for the non-coated and ALD-HA-coated titanium substrates. No significant difference in the speed of blood coagulation was observed between the substrates.

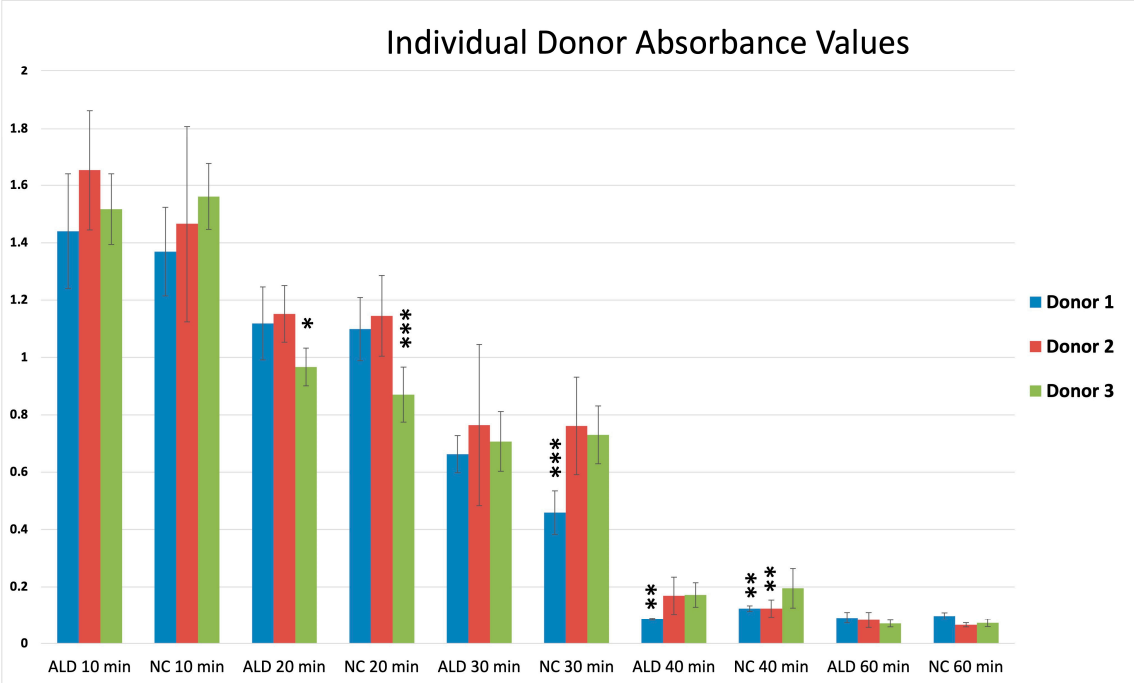

Figure 6. Mean (±SD) optical density (OD) at 570 nm vs. time for the non-coated and ALD-HA-coated titanium substrates for the individual donors. * $p < 0.05$, ** $p < 0.01$, *** $p < 0.001$.

3.4. Platelets' Adhesion and Morphology

Platelets adhered on both non-coated and ALD-HA-coated surfaces, as seen from SEM images after a 1 h adhesion period (Figure 7). Visualization of the platelet adhesion indicated that the ALD-HA-coated surfaces seem to have more platelets compared to the

non-coated surfaces. Also, there was variability in the platelet morphologies in different areas. The platelets on the non-coated substrates maintained their round or dendritic shape, indicating a lower activation state. In contrast, the ALD-HA-coated substrates showed a different platelet morphology with a greater platelet transformation to dendritic shape and early pseudopodial spread. Also, some platelets with filopodia extended to form a connection with each other, which indicates a higher activation state.

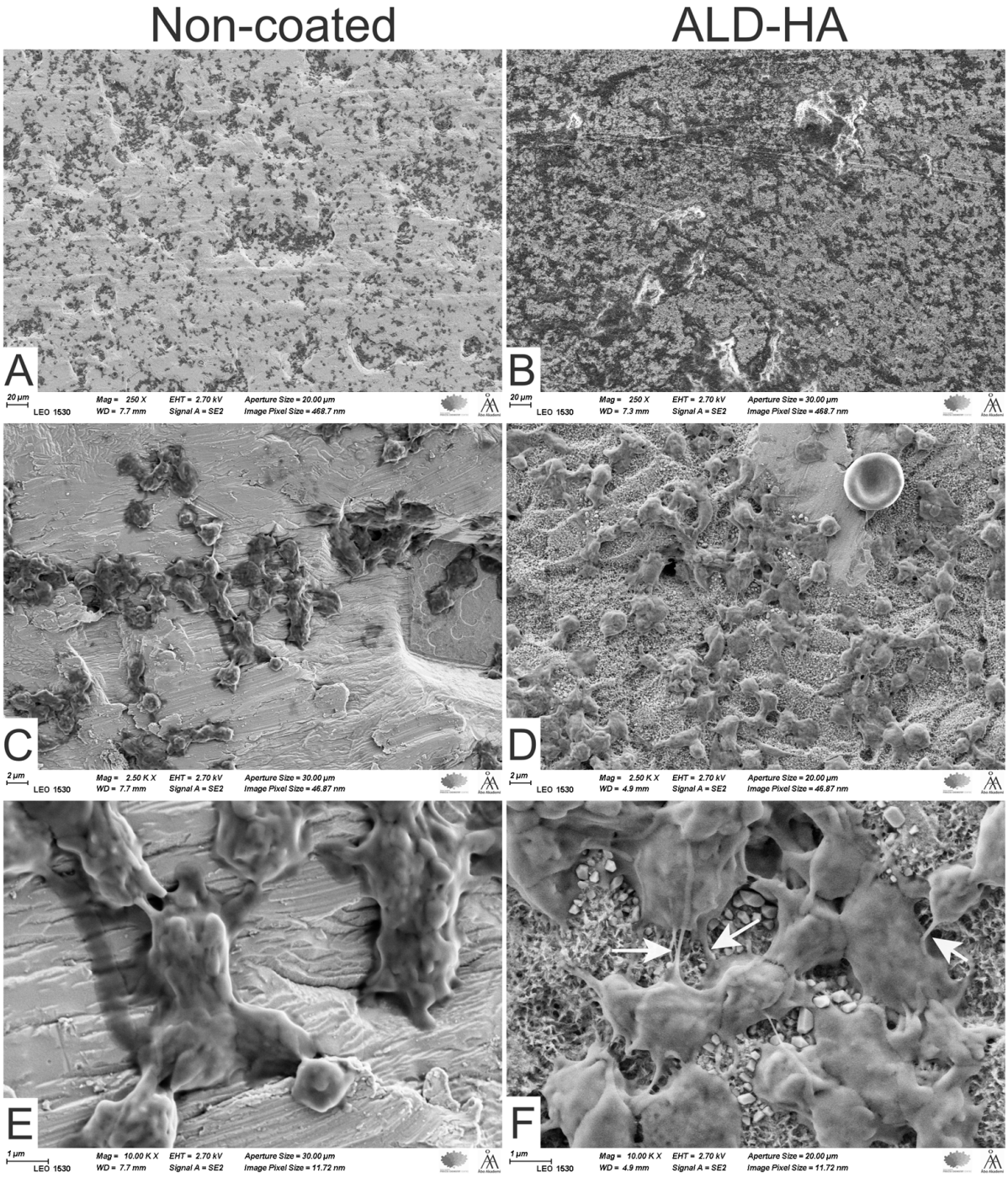

Figure 7. Scanning electron microscopic images of platelet morphologies after 1 h adhesion period on the non-coated (**A**,**C**,**E**) and ALD-HA-coated (**B**,**D**,**F**) titanium substrates. Magnifications 250× (**A**,**B**), 2500× (**C**,**D**), and 10,000× (**E**,**F**). Arrows in (**F**) indicate the dendrites connecting the platelets.

4. Discussion

Chemical surface modifications play an important role in the performance of endosseous implants [23]. This study evaluated the influence of an ALD-HA coating on titanium on blood coagulation and platelet adhesion. The results indicated that whole-blood coagulates and the platelets adhere to the ALD-HA-coated titanium in a similar manner as the non-coated titanium surface does.

The success of implant osseointegration largely depends on the interaction between blood and the implant surface, leading to coagulation [24]. When the blood comes into contact with the implant surface, it triggers various complex events such as protein adsorption, platelet formation, and coagulation. Blood clot formation is crucial for the healing process of surgical wounds and subsequent tissue growth during osseointegration [25–27]. A blood clot forms a natural barrier, preventing wound infection, and thus plays a critical role in the healing process of surgical wounds and subsequent tissue growth during osseointegration [18,19,28]. In our study, the blood coagulation on the substrate surfaces was assessed by measuring the released hemoglobin; more hemoglobin in the solution indicated a lower coagulation speed. A three-donor approach was used to compare the response of the material surface to blood obtained from the different donors. The blood from the individual donors reacted differently on the substrates, indicating a minor variation between the individuals in the coagulation speed, especially in the early stages. However, at 60 min, complete blood coagulation was achieved for all the donors and substrates. These results agree with the previous results from similar blood clotting assays but on different titanium surface coatings [25,29,30], indicating that the ALD-HA coating did not slow the coagulation process.

Based on the criteria described earlier by Goodman et al. [31], the platelet activation patterns ranged from low-activated to high-activated states. According to their criteria, the platelets were categorized into round or discoid cells, dendritic shape, early pseudopodial spread, and full spread. In this study, the adherent platelets on the non-coated substrates were at a lower activated state (discoid). In contrast, the platelets on ALD-HA-coated substrates showed more platelet activation (dendritic and early spread state), indicating a higher activation state than the non-coated substrates. This favorable platelet response could be attributed to the enhanced wettability on the ALD-HA coating compared to the non-coated surfaces.

Water CA and SFE of the surface are important factors for the initial cellular adhesion [32–34]. Generally, a surface with a CA less than 90° is considered hydrophilic, while a surface with a CA higher than 90° is regarded as hydrophobic. SFE has polar (γp) and dispersive (γd) components. The polar component of the SFE has a significant influence on cell behavior. Cells interact with materials mainly in a polar force [35]. The surfaces with high polar SFE components show small contact angles with polar liquids, such as water [29,30]. This increases wettability and enhances cell attachment, thus improving the interaction between the implant surface and the surrounding tissues [30,36]. Results of the present study indicate that the ALD-HA-coated surface has a significantly higher wettability and polar SFE than the non-coated surface, but there is no difference in the total SFE between the two samples. Higher wettability may explain the favorable platelet adhesion on the ALD-HA coating compared to the non-coated surfaces, as seen in the difference in platelet morphologies.

The presence of Ca and P elements on the ALD-HA-coated surfaces might also explain the favorable platelet adhesion. However, these results are inconsistent with findings from similar studies, which reported that surfaces with low CA showed isolated smaller quantities of adhered platelets [36–38]. In addition, Kikuchi and co-workers [38] reported that platelet adhesion is similar on acid-etched titanium surfaces, and HA is produced by an organic sol using triethyl phosphite or inorganic sol. The authors claimed that the surface microtopography is responsible for platelet activation rather than the presence of Ca and PO4 on the surface. In the present study, platelet adhesion was qualitatively evaluated from observations on SEM images. The higher platelet density, as indicated by

morphology, observed on the ALD-HA-coated surface did not influence the speed of blood coagulation on the surface.

Increased surface roughness at the nanoscale level has been reported to enhance platelet adhesion and blood coagulation [29,39]. However, BhavanChand and co-workers [40] reported contradicting results that surface roughness does not influence platelet adhesion. On the other hand, our study showed that platelets could adhere on both surfaces with slightly more preference for the ALD-HA-coated surfaces, which had lower surface roughness. Platelets on ALD-HA-coated surfaces exhibited an activated morphology as indicated by their spreading and extended pseudopodia. A similar extended morphology with long filopodia has also been observed for MC3T3 cells cultured on ALD-HA-coated surfaces [16].

Therefore, a quantitative platelet adhesion assay with more detailed data about cell adhesion may be necessary to evaluate the real significance between the ALD-HA-coated and non-coated titanium surfaces in this respect.

5. Conclusions

Within the limitations of this study, it may be concluded that the nanocrystalline hydroxyapatite coating obtained through the atomic layer deposition method can support blood coagulation and platelet response on the titanium surface. The coating can also reduce the surface roughness of the titanium and enhance the surface wettability and the polar component of the surface free energy.

Author Contributions: Conceptualization: F.A., J.H., M.R., J.T. and T.N.; Methodology: F.A., N.A., J.H., M.R. and T.N.; Sample Preparation: J.H. and M.R.; Resources: E.K., L.H. and J.T.; Formal Analysis: F.A.; Investigation: F.A. and N.A.; Data Curation: F.A.; Writing—Original Draft Preparation: F.A.; Writing—Review and Editing: N.A., E.K., J.H., M.R., L.H., J.T. and T.N.; Visualization: F.A. and N.A.; Supervision: T.N. All authors have read and agreed to the published version of the manuscript.

Funding: This research received no external funding.

Institutional Review Board Statement: Not applicable.

Informed Consent Statement: Not applicable.

Data Availability Statement: Not applicable.

Acknowledgments: Biomedical research technician Katja Sampalahti is kindly acknowledged for her technical assistance in the laboratory.

Conflicts of Interest: The authors declare that this paper is original and free of any conflicts of interest.

References

1. Albrektsson, T.; Brånemark, P.-I.; Hansson, H.-A.; Lindström, J. Osseointegrated titanium implants: Requirements for ensuring a long-lasting, direct bone-to-implant Anchorage in man. *Acta Orthop. Scand.* **1981**, *52*, 155–170. [CrossRef] [PubMed]
2. Mints, D.; Elias, C.; Funkenbusch, P.; Meirelles, L. Integrity of implant surface modifications after insertion. *Int. J. Oral Maxillofac. Implants* **2014**, *29*, 97–104. [CrossRef]
3. Buser, D.; Broggini, N.; Wieland, M.; Schenk, R.K.; Denzer, A.J.; Cochran, D.L.; Hoffmann, B.; Lussi, A.; Steinemann, S. Enhanced bone apposition to a chemically modified SLA titanium surface. *J. Dent. Res.* **2004**, *83*, 529–533. [CrossRef] [PubMed]
4. Jeffcoat, M.K.; McGlumphy, E.A.; Reddy, M.S.; Geurs, N.C.; Proskin, H.M. A comparison of hydroxyapatite (HA)-coated threaded, HA-coated cylindric, and titanium threaded endosseous dental implants. *Int. J. Oral Maxillofac. Implants* **2003**, *18*, 406–410. [CrossRef]
5. Porter, A.E.; Hobbs, L.W.; Rosen, V.B.; Spector, M. The ultrastructure of the plasma-sprayed hydroxyapatite-bone interface predisposing to bone bonding. *Biomaterials* **2022**, *23*, 725–733. [CrossRef]
6. Mohseni, E.; Zalnezhad, E.; Bushroa, A.R. Comparative investigation on the adhesion of hydroxyapatite coating on Ti-6Al-4V implant: A review paper. *Int. J. Adhes. Adhes.* **2014**, *48*, 238–257. [CrossRef]
7. Coathup, M.J.; Blunn, G.W.; Flynn, N.; Williams, C.; Thomas, N.P. A comparison of bone remodelling around hydroxyapatite-coated, porous-coated and grit-blasted hip replacements retrieved at post-mortem. *J. Bone Jt. Surg. Br. Ser. B* **2001**, *83*, 118–123. [CrossRef]
8. Jeong, J.; Kim, J.H.; Shim, J.H.; Hwang, N.S.; Heo, C.Y. Bioactive calcium phosphate materials and applications in bone regeneration. *Biomater. Res.* **2019**, *23*, 4. [CrossRef] [PubMed]

9. Yang, Y.; Liu, Z.; Luo, C.; Chuang, Y. Measurements of residual stress and bond strength of plasma sprayed laminated coatings. *Surf. Coat. Technol.* **1997**, *89*, 97–100. [CrossRef]
10. Gross, K.A.; Berndt, C.C.; Herman, H. Amorphous phase formation in plasma-sprayed hydroxyapatite coatings. *J. Biomed. Mater. Res.* **1998**, *39*, 407–414. [CrossRef]
11. Heimann, R.B. Plasma-Sprayed Hydroxylapatite-Based Coatings: Chemical, Mechanical, Microstructural, and Biomedical Properties. *J. Therm. Spray Technol.* **2016**, *25*, 827–850. [CrossRef]
12. Astaneh, S.H.; Faverani, L.P.; Sukotjo, C.; Takoudis, C.G. Atomic layer deposition on dental materials: Processing conditions and surface functionalization to improve physical, chemical, and Clinical Properties—A Review. *Acta Biomater.* **2021**, *121*, 103–118. [CrossRef] [PubMed]
13. Holopainen, J.; Kauppinen, K.; Mizohata, K.; Santala, E.; Mikkola, E.; Heikkilä, M.; Kokkonen, H.; Leskelä, M.; Lehenkari, P.; Tuukkanen, J.; et al. Preparation and bioactive properties of nanocrystalline hydroxyapatite thin films obtained by conversion of atomic layer deposited calcium carbonate. Biointerphases. *Biointerphases* **2014**, *9*, 031008. [CrossRef] [PubMed]
14. Avila, I.; Pantchev, K.; Holopainen, J.; Ritala, M.; Tuukkanen, J. Adhesion and mechanical properties of nanocrystalline hydroxyapatite coating obtained by conversion of atomic layer-deposited calcium carbonate on titanium substrate. *J. Mater. Sci. Mater. Med.* **2018**, *29*, 11. [CrossRef]
15. Reyes, C.D.; Petrie, T.A.; Burns, K.L.; Schwartz, Z.; García, A.J. Biomolecular surface coating to enhance orthopaedic tissue healing and integration. *Biomaterials* **2007**, *28*, 3228–3235. [CrossRef]
16. Kylmäoja, E.; Holopainen, J.; Abushahba, F.; Ritala, M.; Tuukkanen, J. Osteoblast attachment on titanium coated with hydroxyapatite by atomic layer deposition. *Biomolecules* **2022**, *12*, 654. [CrossRef]
17. Kylmäoja, E.; Abushahba, F.; Holopainen, J.; Ritala, M.; Tuukkanen, J. Monocyte differentiation on atomic layer-deposited (ALD) hydroxyapatite coating on titanium substrate. *Molecules* **2023**, *28*, 3611. [CrossRef] [PubMed]
18. Park, J.Y.; Davies, J.E. Red blood cell and platelet interactions with titanium implant surfaces. *Clin. Oral Implants Res.* **2000**, *11*, 530–539. [CrossRef]
19. Davies, J.E. Understanding peri-implant endosseous healing. *J. Dent. Educ.* **2003**, *67*, 932–949. [CrossRef]
20. Nilsen, O.; Fjellvåg, H.; Kjekshus, A. Growth of calcium carbonate by the atomic layer chemical vapour deposition technique. *Thin Solid Films* **2004**, *450*, 240–247. [CrossRef]
21. de Jong, H.P.; van Pelt, A.W.J.; Arends, J. Contact angle measurements on human enamel—An in vitro study of influence of pellicle and storage period. *J. Dent. Res.* **1982**, *61*, 11–13. [CrossRef]
22. Abdulmajeed, A.A.; Walboomers, X.F.; Massera, J.; Kokkari, A.K.; Vallittu, P.K.; Närhi, T.O. Blood and fibroblast responses to thermoset BisGMA-TEGDMA/glass fiber-reinforced composite implants in vitro. *Clin. Oral Implant. Res.* **2014**, *25*, 843–851. [CrossRef] [PubMed]
23. Bauer, S.; Schmuki, P.; Von Der Mark, K.; Park, J. Engineering biocompatible implant surfaces. *Prog. Mater. Sci.* **2012**, *58*, 261–326.
24. Gittens, R.A.; Olivares-Navarrete, R.; Schwartz, Z.; Boyan, B.D. Implant osseointegration and the role of microroughness and nanostructures: Lessons for spine implants. *Acta Biomater.* **2014**, *10*, 3363–3371. [CrossRef]
25. Gorbet, M.B.; Sefton, M.V. Biomaterial-associated thrombosis: Roles of coagulation factors, complement, platelets and leukocytes. *Biomaterials* **2004**, *25*, 5681–5703. [CrossRef]
26. Gear, A.R.; Camerini, D. Platelet chemokines and chemokine receptors: Linking hemostasis, inflammation, and host defense. *Microcirculation* **2003**, *10*, 335–350. [CrossRef]
27. Toma, A.I.; Fuller, J.M.; Willett, N.J.; Goudy, S.L. Oral wound healing models and emerging regenerative therapies. *Transl. Res.* **2021**, *236*, 17–34. [CrossRef] [PubMed]
28. Milillo, L.; Cinone, F.; Presti, F.L.; Lauritano, D.; Petruzzi, M. The Role of Blood Clot in Guided Bone Regeneration: Biological Considerations and Clinical Applications with Titanium Foil. *Materials* **2021**, *14*, 6642. [CrossRef]
29. Xu, L.C.; Bauer, J.W.; Siedlecki, C.A. Proteins, platelets, and blood coagulation at biomaterial interfaces. *Colloids Surf. B Biointerfaces* **2014**, *124*, 49–68. [CrossRef]
30. Kligman, S.; Ren, Z.; Chung, C.H.; Perillo, M.A.; Chang, Y.C.; Koo, H.; Zheng, Z.; Li, C. The Impact of Dental Implant Surface Modifications on Osseointegration and Biofilm Formation. *J. Clin. Med.* **2021**, *10*, 1641. [CrossRef] [PubMed]
31. Goodman, S.L.; Lelah, M.D.; Lambrecht, L.K.; Cooper, S.L.; Albrecht, R.M. In vitro vs. ex vivo platelet deposition on polymer surfaces. *Scanning Electron Microsc.* **1984**, *1*, 279–290.
32. Ostrovskaya, L.; Perevertailo, V.; Ralchenko, V.; Dementjev, A.; Loginova, O. Wettability and surface energy of oxidized and hydrogen plasma-treated diamond films. *Diam. Relat. Mater.* **2002**, *11*, 845–850. Available online: https://www.sciencedirect.com/science/article/pii/S0925963501006367 (accessed on 3 April 2023). [CrossRef]
33. Kilpadi, D.V.; Lemons, J.E. Surface energy characterization of unalloyed titanium implants. *J. Biomed. Mater. Res.* **1994**, *28*, 1419–1425. [CrossRef] [PubMed]
34. PeŠŠková, V.; Kubies, D.; Hulejová, H.; Himmlová, L. The influence of implant surface properties on cell adhesion and proliferation. *J. Mater. Sci. Mater. Med.* **2007**, *18*, 465–473. [CrossRef] [PubMed]
35. Feng, B.; Weng, J.; Yang, B.C.; Qu, S.X.; Zhang, X.D. Characterization of surface oxide films on titanium and adhesion of osteoblast. *Biomaterials* **2003**, *24*, 4663–4670. [CrossRef]
36. Riivari, S.; Shahramian, K.; Kangasniemi, I.; Willberg, J.; Närhi, T.O. TiO_2-Modified Zirconia Surface Improves Epithelial Cell Attachment. *Int. J. Oral Maxillofac. Implants* **2019**, *34*, 313–319. [CrossRef] [PubMed]

37. Jones, M.I.; McColl, I.R.; Grant, D.M.; Parker, K.G.; Parker, T.L. Protein adsorption and platelet attachment and activation, on TiN, TiC, and DLC coatings on titanium for cardiovascular applications. *J. Biomed. Mater. Res.* **2000**, *52*, 413–421. [CrossRef]
38. Kikuchi, L.; Park, J.Y.; Victor, C.; Davies, J.E. Platelet interactions with calcium-phosphate-coated surfaces. *Biomaterials* **2005**, *26*, 5285–5295. [CrossRef]
39. Zhang, L.; Liao, X.; Fok, A.; Ning, C.; Ng, P.; Wang, Y. Effect of crystalline phase changes in titania (TiO_2) nanotube coatings on platelet adhesion and activation. *Mater. Sci. Eng. C Mater. Biol. Appl.* **2018**, *82*, 91–101. [CrossRef] [PubMed]
40. BhavanChand, Y.; Ranzani, R.; Annapoorani, H. Evaluation of Hemocompatibility of Titanium after Various Surface Treatments: An in vitro Study. *Int. J. Prosthodont. Restor. Dent.* **2012**, *2*, 136–142.